

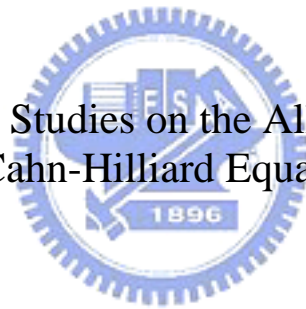
國立交通大學

應用數學系

碩士論文

Allen-Cahn 與 Cahn-Hilliard 方程的數值研究

Numerical Studies on the Allen-Cahn and
Cahn-Hilliard Equations



研究生：陳冠羽

指導教授：賴明治 教授

中華民國九十六年七月

Allen-Cahn 與 Cahn-Hilliard 方程的數值研究

Numerical Studies on the Allen-Cahn and
Cahn-Hilliard Equations

研 究 生：陳冠羽

Student : Kuan-Yu Chen

指 導 教 授：賴明治

Advisor : Ming-Chih Lai

國立交通大學
應用數學系
碩士論文



Submitted to Department of Applied Mathematics

College of Science

National Chiao Tung University

in partial Fulfillment of the Requirements

for the Degree of

Master

in

Applied Mathematics

July 2007

Hsinchu, Taiwan, Republic of China

中華民國九十六年七月


Allen-Cahn 與 Cahn-Hilliard 方程 的數值研究

學生：陳冠羽

指導教授：賴明治

國立交通大學應用數學系（研究所）碩士班

摘 要



本論文介紹計算 Allen-Cahn 方程的一個簡單快速且穩定的有限差分算法，只需要解一個三條對角線的線性方程，並利用本方法做調整來解 Cahn-Hilliard 方程。我們也介紹一套利用快速傅立葉轉換的優點來計算 Allen-Cahn 方程的分離算法。我們修正了 Allen-Cahn 方程原本質量不守衡的問題，並且將這套方法應用在不可壓縮的兩項流混合問題上。

Numerical Studies on the Allen–Cahn and Cahn–Hilliard Equations

Student : Kuan-Yu Chen

Advisor: Ming-Chih Lai

Department (Institute) of Applied Mathematics

National Chiao Tung University



Abstract

We propose simple finite difference schemes with fast and stable computations for the Allen-Cahn equation with solving tri-diagonal matrices. We also deal this with the Cahn-Hilliard equation in a similar way. We introduce a special splitting method for the Allen-Cahn equation in advantage of applying fast Fourier transform. Mass-conservation modification for the Allen-Cahn equation is provided. And we apply these methods to compute the mixture problem of two incompressible fluids.

誌 謝

本篇論文的完成，首先要感謝我的指導老師—賴明治教授。在老師的指點之下，讓我逐漸熟悉數值偏微分方程與科學計算等領域，並且引導我學習與研究的方向。除了課業上的知識以外，老師也讓我學到許多求知與做研究的方法，讓我在數值方法與科學計算這片領域中，找到我的興趣跟做出研究的成就感。除了指導老師外，科學計算實驗室的夥伴們也給我不少幫助。感謝曾昱豪學長指點我 Allen-Cahn、Cahn-Hilliard 和 Navier-Stokes 方程的理論和數值計算，讓我在研究的過程中能夠持續獲得進展，也在尋找研究資料時給我許多幫助。感謝曾孝捷學長指點我程式和學業，讓我在撰寫程式時更加得心應手，課業上迷惑時能有適時的引導，尤其是論文後半段的應用部分，特別要感謝他的細心提點。感謝吳恭儉學長以他雄厚的分析能力給我在理論方面的幫助，也感謝許多已經畢業的學長姐留下來的資料。學生在此致上最誠懇的謝意。

在論文口試期間，承蒙楊肅煜副教授、洪子倫副教授與鄭博文助理教授費心審閱並提供許多寶貴意見，使本論文得以更加完備，學生永銘在心。



除了研究生活外，我也要感謝陳偉國學長、涂芳婷學姊、楊川和學長、胡仲軒同學以及其他碩一學弟。除了課業上的切磋討論外，閒暇之餘能跟他們閒話家常，交換各種意見與心得，讓我的生活充滿樂趣，在互相鼓勵之下度過研究所的生涯。

最後，我要感謝我的家人，沒有他們的關心與祝福，我無法順利的完成學業。願與他們，以及所有在我周圍關心我的人，一同分享此篇論文完成之喜悅與榮耀。

目 錄

中文提要	i
英文提要	ii
誌謝	iii
目錄	iv
一、	Introduction	1
二、	Numerical Methods of the Allen-Cahn Equations ...	2
2.1	Gradient Stable Crank-Nicolson Adams-Bashforth Scheme	3
2.2	Mass Conservation	3
2.3	Gilbert-Strang Splitting Scheme	4
三、	Numerical Methods of the Cahn-Hilliard Equations	6
3.1	Gradient Stable Crank-Nicolson Adams-Bashforth Scheme	7
四、	Numerical Results	8
4.1	Smooth Initial Data	8
4.2	Square Block Initial Data	14
五、	Application of the Allen-Cahn and Cahn-Hilliard Equations	18
5.1	Mixture of Two Incompressible Fluids	18
5.2	Numerical Scheme for Coupled System	18
5.3	Computing Mixture Problems Using Phase Field Models	21
六、	Conclusion	22
Reference	22

1 Introduction

In this paper, we consider the interface problems in mixture of two incompressible fluids. Instead of taking into account the position of interface, we adapt the phase functions to describe the distribution of different fluids. We will provide fast, stably numerical schemes to treat these problems. And we also present the application of phase field model on mixture of fluids with our numerical methods.

The method of phase function is originally proposed by Cahn and Hilliard [3] in 1950's. In order to prevent calculating complex geometry of the interface, they use the phase function to describe the distribution of different alloys derived from the interfacial free energy in a nonuniform system. The Cahn-Hilliard equation for the phase function can be derived by the relation between interface velocity and the Laplacian of variational derivative of the interfacial free energy. In computation of Cahn-Hilliard equation, Elliot, et al. [5, 6] propose a second order finite element Galerkin method in the late 1980's. Furihata [8, 9] introduce a stable finite different scheme in 2001 and 2003.

In 1970's, Allen and Cahn [1] used simplified phase field models for describing Fe-Al alloys system. The Laplacian of variational derivative of the interfacial free energy is substituted by variational derivative itself. The Allen-Cahn equation is easier to compute but lack of mass conservation. Carr and Pego [4] proved the metastability for Allen-Cahn equation in 1989. Ward, et al. [15, 16] provide an asymptotic approximation solution for the Allen Cahn equation in 1990's.

For the stability of numerical schemes, Eyre [7] propose gradient stable discretization for numerical methods, and Vollmayr-Lee and Rutenberg [14] provide unconditional stable scheme derived from Eyre's work.

To deal with mixture of two incompressible fluids, Authors of [2, 10, 17] couple the Navier-Stokes equation with Allen-Cahn and Cahn-Hilliard equations. They use finite element / multigrid schemes to compute the dynamics of interface problems.

In the rest of this paper, numerical schemes for the Allen-Cahn equation will propose in Section 2, while methods to the Cahn-Hilliard equation will be introduced in Section 3. Some numerical results will be shown in Section 4. The application of phase field models will be presented in section 5 before we conclude with a summary in Section 6.

2 Numerical Methods of the Allen-Cahn Equation

We consider the Allen-Cahn equation in a well-behaved domain $\Omega \times [0, \infty)$. The governing equation is written as following :

$$\frac{\partial}{\partial t} \Phi = \epsilon^2 \Delta \Phi + f(\Phi) \quad (1)$$

Here $\Phi(x, t)$ is the phase function of two kinds of liquid. For $\Phi(x_1, t_1) = 1$, it means that at the time t_1 , the position x_1 is filled only one kind of liquid; for $\Phi(x_2, t_2) = -1$, it means that at the time t_2 , the position x_2 is filled only the other kind of liquid. Hence $\Phi(x, t) \in [-1, 1]$. The ϵ here is a small positive constant, which is related to the width of the interface of two kinds of liquid. For $t = 0$, we shall give the initial data $\Phi(x, 0) = \Phi_0(x)$.

The term $\epsilon^2 \Delta \Phi$ represents the diffusion of the liquid, and the term $f(\Phi)$ is the kinetic potential of the liquid. Here, for example, we use the double-well potential $f(\Phi) = \Phi(1 - \Phi^2)$, which means that Φ tends to be 1 or -1 by simple equilibrium analysis of differential equations.

Since the spatial boundary is of no flux, we may consider the Neumann boundary condition at the boundary $\partial\Omega$, i.e.

$$\frac{\partial \Phi}{\partial \mathbf{n}}(x, t) = 0 \text{ for } x \in \partial\Omega \quad (2)$$

In order to calculate the solution near the boundary easily, we use a stagger grid on the domain Ω , which means that the solution of Φ is computed on the cell center.

The Allen-Cahn equation has the following properties :

Property 1. No mass conservation

The mass function of the Allen-Cahn equation is defined as

$$M(\Phi)(t) = \frac{1}{\text{vol}(\Omega)} \int_{\Omega} \Phi(x, t) dx \quad (3)$$

The Allen-Cahn equation does not obey mass conservation. i.e.

$$\frac{d}{dt} M(\Phi) \neq 0 \quad (4)$$

Property 2. Energy decreasing

The energy function of the Allen-Cahn equation is defined as

$$G(\Phi)(t) = \int_{\Omega} \left(\frac{(1 - \Phi^2)^2}{4} + \frac{\epsilon^2}{2} \left(\frac{\partial \Phi}{\partial x} \right)^2 \right) dx \quad (5)$$

The energy function of Allen-Cahn equation is decreasing as time t increases. i.e.

$$\frac{d}{dt} G(\Phi) \leq 0 \quad (6)$$

Note that the Allen-Cahn equation is derived from energy. By using the technique of calculus of variations, we can obtain the terms $\epsilon^2 \Delta \Phi + f(\Phi)$ from the Euler-Lagrange equation of $\partial G / \partial \Phi$.

Property 3. Phase Separation

When the time t is large enough, the graph of $\Phi(x, t_0)$ will show the combination of intervals of $\Phi(x, t_0) = 1$ and $\Phi(x, t_0) = -1$ at the time $t = t_0$.

Property 4. The "Metastable" phenomenon

In the time evolution of the Allen-Cahn equation, the graph of $\Phi(x, t)$ will has some "stable state" in short period and transform to another state dramatically.

2.1 Gradient Stable Crank-Nicolson Adams-Bashforth Scheme

First, we introduce the Crank-Nicolson Adams-Bashforth scheme for 1-D case. We use $\frac{\Phi^{n+1} - \Phi^n}{\Delta t}$ to approximate Φ_t on the time $t = (n + 1/2)\Delta t$. Then we apply the Crank-Nicolson scheme to the diffusion term $\epsilon^2 \frac{\partial^2}{\partial x^2} \Phi$ to approximate on the time $t = (n + 1/2)\Delta t$. Finally, we want to approximate $f(\Phi)$ in a similar manner. To avoid solving a nonlinear equation, we adapt Adams-Bashforth scheme to extrapolate the nonlinear term $f(\Phi)$. The scheme is written as below:

$$\begin{aligned} \frac{\Phi^{n+1} - \Phi^n}{\Delta t} &= \frac{\epsilon^2}{2} (\Delta \Phi^{n+1} + \Delta \Phi^n) \\ &+ \frac{1}{2} (-2\Phi^{n+1} - 2\Phi^n + 3(3\Phi^n - (\Phi^n)^3) - (3\Phi^{n-1} - (\Phi^{n-1})^3)) \end{aligned}$$

To increase the stability of the scheme, we put the additional $\Phi^{n-1}, \Phi^n, \Phi^{n+1}$ into our scheme. This idea comes from the gradient stability, see Eyre's [7].

During calculating the Allen-Cahn equation by this method, we need to solve a linear system with a constant tri-diagonal matrix in one dimension, or a constant block tri-diagonal matrix in higher dimensions. With explicitly computing the nonlinear term, these procedures are cheap. This method is numerically stable under the condition that $\Delta t \leq 0.1$ and $\Delta x \leq 0.2$.

2.2 Mass Conservation

Since the Allen-Cahn equation does not satisfy mass-conservation property, we may insert an additional equation for mass-conservation into the original Allen-Cahn equation:

$$\frac{\partial}{\partial t} \Phi = \epsilon^2 \Delta \Phi + f(\Phi) \tag{7}$$

with the boundary conditions, initial conditions

$$\begin{aligned} \frac{\partial \Phi}{\partial \mathbf{n}} &= 0 \\ \Phi(x, 0) &= \Phi_0(x) \end{aligned} \tag{8}$$

and the mass-conserved condition

$$\frac{d}{dt} \frac{1}{\text{vol}(\Omega)} \int_{\Omega} \Phi(x, t) dx = 0 \quad \forall t \quad (9)$$

Hence we may consider the modified Allen-Cahn equation:

$$\frac{\partial}{\partial t} \Phi = \epsilon^2 \frac{\partial^2}{\partial x^2} \Phi + f(\Phi) - \sigma(t) \quad (10)$$

with the same boundary and initial conditions. In this case, σ is a function for mass modification, analog to the Lagrange multiplier.

2.3 Gilbert Strang Splitting Scheme

For this problem, we introduce the **Gilbert Strang splitting scheme**.

The idea of applying this method comes from [11]. We rewrite the Allen-Cahn equation as below

$$\frac{\partial}{\partial t} \Phi = L\Phi + F\Phi \quad (11)$$

where L and F are operators of Φ . In theories of ordinary differential equations, if we can write L and F as matrices, we have

$$\Phi = \exp((L + F)t)\Phi_0 \quad (12)$$

If L and F are commutative, then we have $\Phi = \exp((L + F)t)\Phi_0 = \exp(Lt)(\exp(Ft)\Phi_0)$. From this idea, we use $\exp(Ft/2)(\exp(Lt)(\exp(Ft/2)))$ to approximate $\exp((L + F)t)$, and this leads to the **Gilbert Strang splitting scheme**.

The whole procedures are stated as following :

Step 1. We need to solve the nonlinear term $\frac{\partial}{\partial t} \Phi = f(\Phi)$ at each grid point x_i by half time step. In our case, since $f(\Phi) = \Phi(1 - \Phi^2)$, the ordinary differential equation above can be solved analytically. By multiple 2Φ at both sides and letting $\Psi = \Phi^2$, we obtain

$$\frac{d}{dt} \Psi = 2\Psi(1 - \Psi) \quad (13)$$

By separation of variables, we have

$$\int_{\Omega} \left(\frac{1}{\Psi} - \frac{1}{\Psi - 1} \right) d\Psi = \int_{t_0}^t 2d\tau \quad (14)$$

After integration, we obtain

$$\ln\left(\frac{\Psi}{\Psi - 1}\right) = 2t + C \quad (15)$$

And the solution of Ψ can be written in the form:

$$\Psi(x, t) = \frac{1}{\frac{\Psi_0}{\Psi_0 - 1} \exp(2t) - 1} = \frac{\Psi_0}{\Psi_0 - (\Psi_0 - 1) \exp(-2t)} \quad (16)$$

where $\Psi_0 = \Psi(x, t_0)$.

Hence for Φ , we have

$$\frac{d}{dt}\Phi = \Phi(1 - \Phi^2) = \Phi(1 - \Psi) = \Phi\left(1 - \frac{\Psi}{\Psi_0 - (\Psi_0 - 1)\exp(-2t)}\right)$$

By using variables separation, we have

$$\int_{\Omega} \frac{d\Phi}{\Phi} = \int_{t_0}^t \left(1 - \frac{\Psi_0}{\Psi_0 - (\Psi_0 - 1)\exp(-2\tau)}\right) d\tau = \int_{t_0}^t \frac{-(\Psi_0 - 1)\exp(-2\tau)}{\Psi_0 - (\Psi_0 - 1)\exp(-2\tau)} d\tau$$

After integrate both sides, we obtain

$$\ln(\Phi) = -\frac{\ln(\Psi_0 - (\Psi_0 - 1)\exp(-2\tau))}{2} + C$$

And the solution of Φ is written in the form:

$$\Phi(x, t) = \frac{\Phi_0}{\sqrt{\Psi_0 - (\Psi_0 - 1)\exp(-2t)}}$$

where $\Phi_0 = \Phi(x, t_0)$.

Therefore, we obtain our numerical scheme as following

$$\Phi^* = \frac{\Phi^n}{\sqrt{(\Phi^n)^2 - ((\Phi^n)^2 - 1)\exp(-\Delta t)}}$$

for half time step at each grid point.

Step 2. We need to apply the mass-conservation condition for the solution obtained by previous step Φ^* . Due to the property of phase separation, instead of using projections, we adapt using add/minus the weight difference to keep mass-conservation. Since the mass of the modified equation is equal to the mass of initial data, we define the function ρ as

$$\rho(t) = \frac{\int_{\Omega} \Phi(x, t) dx}{\text{vol}(\Omega)} - M \quad (17)$$

where M is the mass of initial data, i.e. $M = \frac{\int_{\Omega} \Phi(x, 0) dx}{\text{vol}(\Omega)}$. For calculating $\rho(t^*)$ for the solution Φ^* , we adapt the following numerical approximation

$$\rho(t^*) = \frac{\sum_{x \in \Omega} \Phi(x, t^*) dx}{\text{vol}(\Omega)} - M$$

Hence the modified solution Φ^{**} can be obtained by

$$\Phi^{**} = \Phi^* - \rho(t^*)$$

Step 3. We need to solve a diffusion equation

$$\frac{\partial}{\partial t}\Phi = \epsilon^2\Delta\Phi \quad (18)$$

Since we have the Neumann boundary conditions, we can adapt the **Fast Cosine Transform** to solve this problem. By the skills of solving ordinary differential equations, we have

$$\widetilde{\Phi}_k^+ = \exp(-\epsilon^2 k^2 \Delta t) \widetilde{\Phi}_k^{**} \quad (19)$$

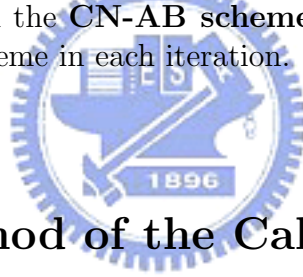
where $\widetilde{\Phi}_k^{**}$ is the k-th Fourier mode of previous step, and $\widetilde{\Phi}_k^+$ is the k-th Fourier mode of the solution to be computed. And then use the **Inverse Fast Cosine Transform** to get the solution Φ^+ .

Step 4. Repeat Step 1. and 2. for the other half time step.

The advantage of this scheme is that we can analytically solve the nonlinear term and use the FCT/IFCT (Fast Cosine Transform/Inverse Fast Fourier Transform) to solve the diffusion term, hence No need to solve any matrix systems.

Since the spatial part reaches spectral accuracy, the order of accuracy depends on the splitting error. In our case, this scheme is second-order accuracy since the splitting error comes from time. In numerical, the time step Δt can be up to 0.5.

Remark. We may modified the **CN-AB scheme** in the same manner. Just apply step 2 after original CN-AB scheme in each iteration.



3 Numerical Method of the Cahn-Hilliard Equation

We consider the Cahn-Hilliard equation in a well-behaved domain $\Omega \times [0, \infty)$. The governing equation is written as following :

$$\frac{\partial}{\partial t}\Phi = \Delta(-\epsilon^2\Delta\Phi - f(\Phi)) \quad (20)$$

Here $\Phi(x, t)$ and ϵ are the same as we defined in Allen-Cahn equation.

Since the spatial boundary is of no flux, we may consider the Neumann boundary condition at $\partial\Omega$, i.e.

$$\frac{\partial}{\partial \mathbf{n}}\Phi(x, t) = \frac{\partial}{\partial \mathbf{n}}\Phi(x, t) = 0 \text{ for } x \in \partial\Omega \quad (21)$$

But note that the Cahn-Hilliard equation contains 4th spatial derivatives since it is bi-harmonic. We need more constraint on the boundary. Let $\mu = \epsilon^2\Delta\Phi + f(\Phi)$, and we may rewrite the Cahn-Hilliard equation as

$$\frac{\partial}{\partial t}\Phi = \Delta(-\mu) \quad (22)$$

Hence we need Neumann boundary condition for μ :

$$\frac{\partial}{\partial \mathbf{n}}\mu(x, t) = \frac{\partial}{\partial \mathbf{n}}\mu(x, t) = 0 \text{ for } x \in \partial\Omega \quad (23)$$

The Cahn-Hilliard equation has the same properties as the Allen-Cahn equation, except which obeys the mass conservation

$$\frac{d}{dt}M(\Phi) = 0 \quad (24)$$

which derived in [8] and [9]. This implies that our numerical results must obey the physical view of mass conservation.

3.1 Gradient stable Crank-Nicolson Adams-Bashforth Scheme

We present our Crank-Nicolson Adams-Bashforth scheme for the Cahn-Hilliard equation in 1-D. First, we define $D = \Delta\Phi$, then the Cahn-Hilliard equation can be written in the form

$$\frac{\partial}{\partial t}\Phi = \Delta(-\epsilon^2 D - f(\Phi)) \quad (25)$$

We use $\frac{\Phi^{n+1} - \Phi^n}{\Delta t}$ to approximate Φ_t on the time $t = (n + 1/2)\Delta t$. Then we apply the Crank-Nicolson scheme to the diffusion term $\Delta(-\epsilon^2 D - f(\Phi))$ to approximate on the time $t = (n + 1/2)\Delta t$. Here, we need another central difference scheme to approximate D^{n+1} implicitly. Similarly, to avoid solving a nonlinear equation, we adapt Adams-Bashforth scheme to extrapolate the nonlinear term $f(\Phi)$. The full scheme is written as below:

$$\frac{\Phi^{n+1} - \Phi^n}{\Delta t} = -\epsilon^2(\Delta D^{n+1} + \Delta D^n) + \frac{1}{2}(2D^{n+1} + 2D^n + 3\Delta\psi^n - \Delta\psi^{n-1})$$

$$\text{where } D^n = \Delta\Phi$$

$$\text{and } \psi^n = (\Phi^n)^3 - 3\Phi^n$$

Again, to increase the stability of the scheme, we put the additional Φ^n into our scheme. This idea comes from the gradient stability, see Eyre's [7].

During calculating the Cahn-Hilliard equation by this method, we need to solve a linear system with a constant block-tri-diagonal matrix, with explicitly computing the nonlinear terms. This scheme is numerically stable under the condition that $\Delta t \leq 0.05$ and $\Delta x \leq 0.5$.

4 Numerical Results

4.1 Example : Smooth Initial Data

We use a modified example from Chapter 13 of [12]. We compute the evolution the Allen-Cahn / Cahn-Hilliard equations on different parameter ϵ with fixed mesh grid size $\Delta x = 0.02$ and time step size $\Delta t = 0.02$. Our calculation domain is $[-1, 1] \times [0, \infty)$. The initial condition is given by

$$\Phi(x, 0) = \Phi_0(x) = 0.53x + 0.47 \sin(-1.5\pi x) \quad (26)$$

and the boundary conditions are Neumann type, i.e.,

$$\frac{\partial}{\partial x} \Phi(-1, t) = \frac{\partial}{\partial x} \Phi(1, t) = 0 \quad (27)$$

for Allen-Cahn equation and

$$\frac{\partial}{\partial x} \Phi(-1, t) = \frac{\partial}{\partial x} \Phi(1, t) = \frac{\partial^3}{\partial x^3} \Phi(-1, t) = \frac{\partial^3}{\partial x^3} \Phi(1, t) = 0 \quad (28)$$

for Cahn-Hilliard equation.

Example 4.1.1 We choose a large parameter $\epsilon^2 = 0.3$. In order to keep the same dynamics, we choose a larger parameter $\epsilon^2 = 0.768$ for the Gilbert Strang splitting scheme. The Allen-Cahn equation has different speed of time-evolution when comparing with that in the Cahn-Hilliard equations. The evolution of phase function are shown in Fig.(1) and (2), which the time increases from right to left. Fig.(3) and (4) are the evolution of mass and energy, respectively, with the time increasing from left to right. In this case, since ϵ is large, the diffusion is more powerful than kinetic potential. Therefore, we can obtain that the phase function is flat, and there is no phase separation during the evolution. Also, since the initial data has mass almost zero, the mass of phase function is still near zero during the computation. Decreasing of energy is obviously shown in figures. The phase function tends to a stable state in a short period.

Example 4.1.2 We choose a smaller parameter $\epsilon^2 = 0.03$ with that in GS method given by $\epsilon^2 = 0.0768$. The evolution of phase function are shown in Fig.(5,6), which the time increases from right to left. Fig.(7,8) are the evolution of mass and energy, respectively, with the time increasing from left to right. Since the diffusion is weaker, kinetic potential has larger effects on the phase function. The phenomenon of phase separation is easy to verify. Metastability is not obvious, we still can observe that the phase function lies in a state in a short period of time during early calculations. The evolution of energy shows the relation between the decreasing of energy and the change of state of the phase function.

Example 4.1.3 Again, we choose a smaller parameter $\epsilon^2 = 0.01$ with that in GS method set by $\epsilon^2 = 0.0256$. The evolution of phase function are shown in Fig.(9,10), which the time increases from right to left. Fig.(11) is the evolution of mass, while Fig.(12,13) are the evolution of energy. The time increases from left to right in the figures of mass and energy. The phase transition shows the metastable phenomenon clearly. The state of phase function is reflected on the evolution of energy. The total time from initial

data to the obvious phase separation behavior is increasing as the parameter ϵ is getting smaller.

Example 4.1.4 We choose a smallest ever parameter $\epsilon^2 = 0.006$ with that in GS method chosen by $\epsilon^2 = 0.01536$. The evolution of phase function are shown in Fig.(14,15), which the time increases from right to left. Fig.(16) is the evolution of mass, while Fig.(17,18) are the evolution of energy. The time increases from left to right in the figures of mass and energy. The evolution of phase function shows that the temporal state of phase, or metastable state, lies in a long period of time after computation initiated. The Cahn-Hilliard equation has more complex behavior during the time of phase transition.

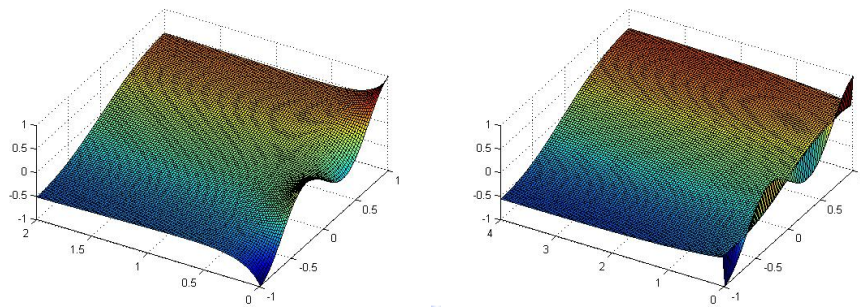


Figure 1: The evolution of phase function of Allen-Cahn (left, CN-AB method, $t=0$ to 2) and Cahn-Hilliard (right, CN-AB method, $t=0$ to 4) equations, $\epsilon^2 = 0.3$

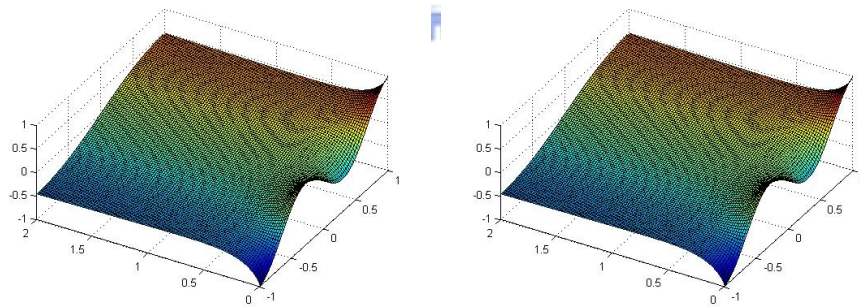


Figure 2: The evolution of phase function of Allen-Cahn (left, GS method, $t=0$ to 2 and right, GS method with mass-conservation, $t=0$ to 2) equation, $\epsilon^2 = 0.768$

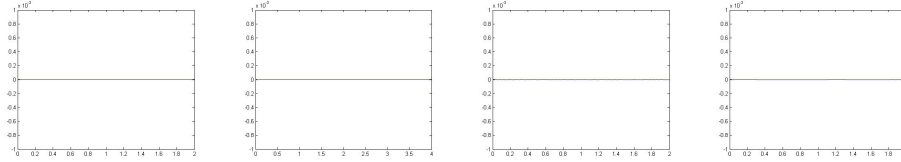


Figure 3: The evolution of mass of Allen-Cahn (left, CN-AB method, $t=0$ to 2, mid-right, GS method, $t=0$ to 2, and right, GS method with mass-conservation, $t=0$ to 2) and Cahn-Hilliard (mid-left, CN-AB method, $t=0$ to 4) equations, scale from -0.001 to 0.001

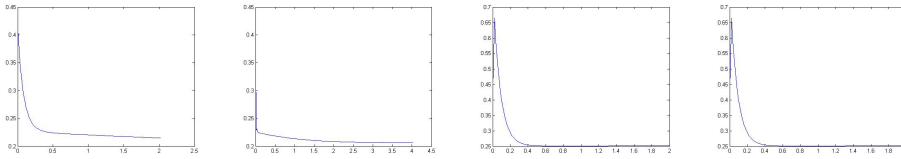


Figure 4: The evolution of energy of Allen-Cahn (left, CN-AB method, $t=0$ to 2, mid-right, GS method, $t=0$ to 2, and right, GS method with mass-conservation, $t=0$ to 2) and Cahn-Hilliard (mid-left, CN-AB method, $t=0$ to 4) equations

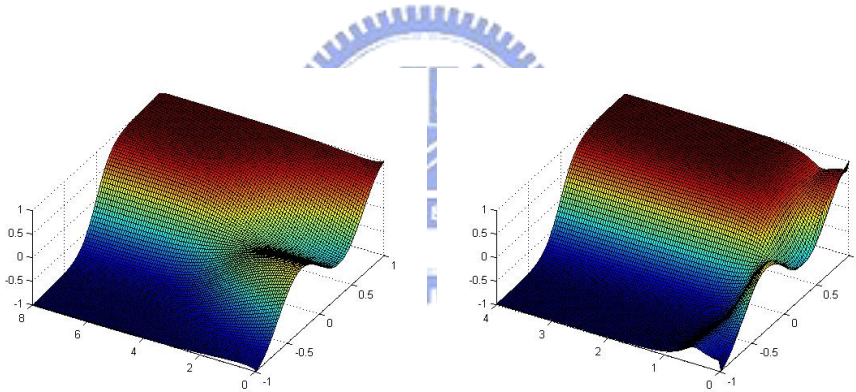


Figure 5: The evolution of phase function of Allen-Cahn (left, CN-AB method, $t=0$ to 8) and Cahn-Hilliard (right, CN-AB method, $t=0$ to 4) equations, $\epsilon^2 = 0.03$

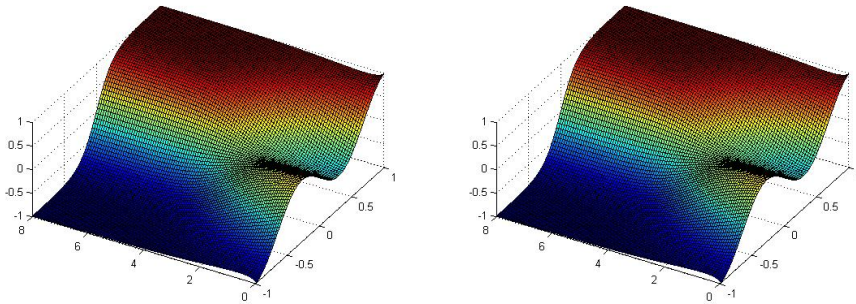


Figure 6: The evolution of phase function of Allen-Cahn (left, GS method, $t=0$ to 8 and right, GS method with mass-conservation, $t=0$ to 8) equation, $\epsilon^2 = 0.0768$

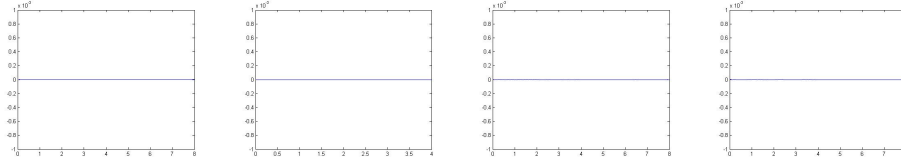


Figure 7: The evolution of mass of Allen-Cahn (left, CN-AB method, $t=0$ to 8, mid-right, GS method, $t=0$ to 8, and right, GS method with mass-conservation, $t=0$ to 8) and Cahn-Hilliard (mid-left, CN-AB method, $t=0$ to 4) equations, scale from -0.001 to 0.001

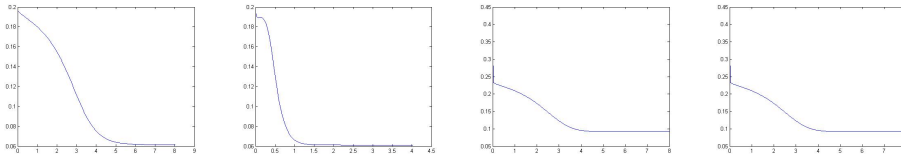


Figure 8: The evolution of energy of Allen-Cahn (left, CN-AB method, $t=0$ to 8, mid-right, GS method, $t=0$ to 8, and right, GS method with mass-conservation, $t=0$ to 8) and Cahn-Hilliard (mid-left, CN-AB method, $t=0$ to 4) equations

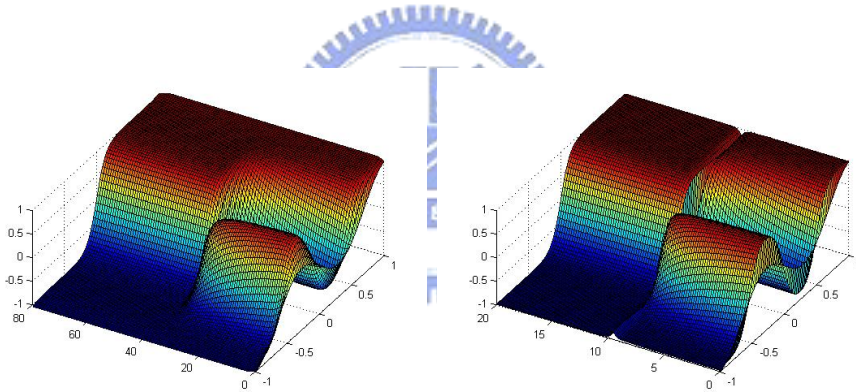


Figure 9: The evolution of phase function of Allen-Cahn (left, CN-AB method, $t=0$ to 80) and Cahn-Hilliard (right, CN-AB method, $t=0$ to 20) equations, $\epsilon^2 = 0.01$

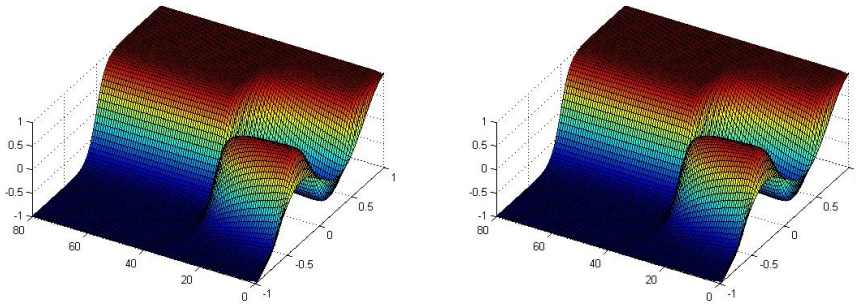


Figure 10: The evolution of phase function of Allen-Cahn (left, GS method, $t=0$ to 80) and right, GS method with mass-conservation, $t=0$ to 80) equation, $\epsilon^2 = 0.0256$

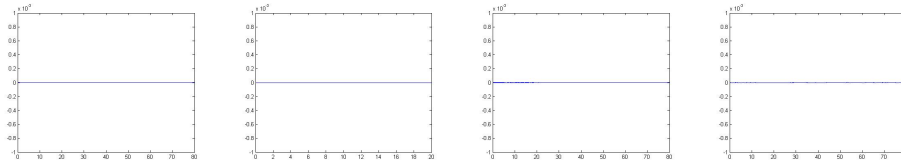


Figure 11: The evolution of mass of Allen-Cahn (left, CN-AB method, $t=0$ to 80, mid-right, GS method, $t=0$ to 80, and right, GS method with mass-conservation, $t=0$ to 80) and Cahn-Hilliard (mid-left, CN-AB method, $t=0$ to 20) equations, scale from -0.001 to 0.001

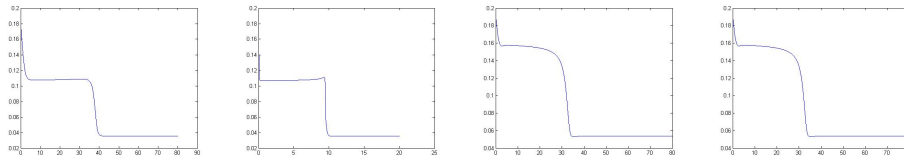


Figure 12: The evolution of energy of Allen-Cahn (left, CN-AB method, $t=0$ to 80, mid-right, GS method, $t=0$ to 80, and right, GS method with mass-conservation, $t=0$ to 80) and Cahn-Hilliard (mid-left, CN-AB method, $t=0$ to 20) equations

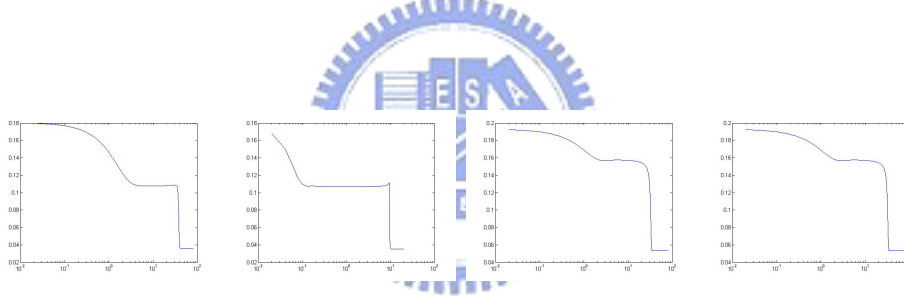


Figure 13: The evolution of energy of Allen-Cahn (left, CN-AB method, $t=0$ to 80, mid-right, GS method, $t=0$ to 80, and right, GS method with mass-conservation, $t=0$ to 80) and Cahn-Hilliard (mid-left, CN-AB method, $t=0$ to 20) equations, log-plot

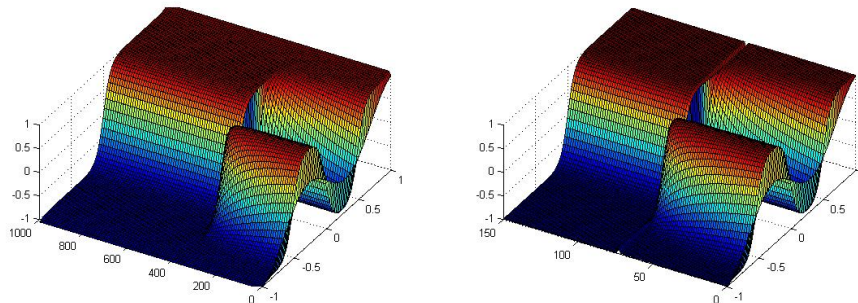


Figure 14: The evolution of phase function of Allen-Cahn (left, CN-AB method, $t=0$ to 1000) and Cahn-Hilliard (right, CN-AB method, $t=0$ to 150) equations, $\epsilon^2 = 0.006$

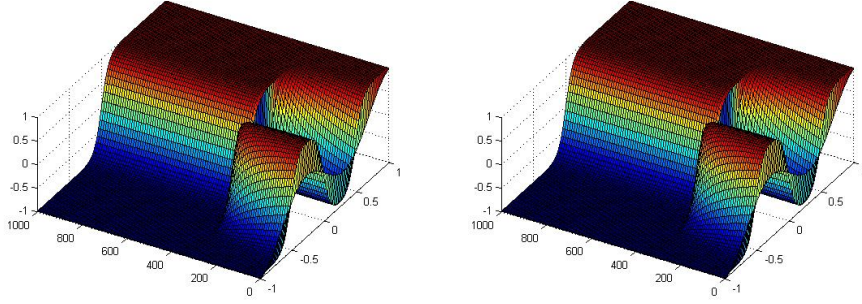


Figure 15: The evolution of phase function of Allen-Cahn (left, GS method, $t=0$ to 1000 and right, GS method with mass-conservation, $t=0$ to 150) equation, $\epsilon^2 = 0.01536$

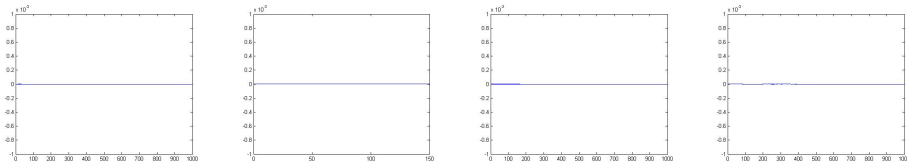


Figure 16: The evolution of mass of Allen-Cahn (left, CN-AB method, $t=0$ to 1000, mid-right, GS method, $t=0$ to 1000, and right, GS method with mass-conservation, $t=0$ to 1000) and Cahn-Hilliard (mid-left, CN-AB method, $t=0$ to 150) equations, scale from -0.001 to 0.001

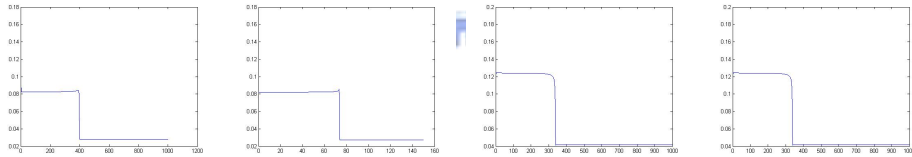


Figure 17: The evolution of energy of Allen-Cahn (left, CN-AB method, $t=0$ to 1000, mid-right, GS method, $t=0$ to 1000, and right, GS method with mass-conservation, $t=0$ to 1000) and Cahn-Hilliard (mid-left, CN-AB method, $t=0$ to 150) equations

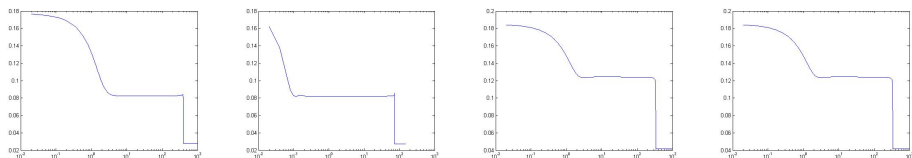


Figure 18: The evolution of energy of Allen-Cahn (left, CN-AB method, $t=0$ to 1000, mid-right, GS method, $t=0$ to 1000, and right, GS method with mass-conservation, $t=0$ to 1000) and Cahn-Hilliard (mid-left, CN-AB method, $t=0$ to 150) equations, log-plot

4.2 Example : Square Block Initial Data

We use a square wave initial data to test our schemes. We compute the evolution the Allen-Cahn equation on fixed parameter $\epsilon^2 = 0.03$ with fixed mesh grid size $\Delta x = 0.02$ and time step size $\Delta t = 0.02$. Our calculation domain is $[-1, 1] \times [0, \infty)$. The initial condition is given by a piecewise constant function with value a on wave crest and value b on wave trough. Again, the boundary conditions are Neumann type, see (27,28).

Example 4.2.1 We choose wave crest $a = 0.8$ and wave trough $b = -0.2$ such that the total mass of initial data is positive. The evolution of phase function are shown in Fig.(19,20), which the time increases from right to left. Fig.(21,22) are the evolution of mass and energy, respectively, with the time increasing from left to right. Since the Allen-Cahn equation does not obey the conservation of mass, We can easily identify that phase function tends to 1.0 as we mentioned in the second section. With mass preserved, the modified Allen-Cahn equation has the same state after long time computation, but less complex behavior during the phase transition between initiation and final state. Since the Cahn-Hilliard equation contains double Laplacian at the right hand side, the interface of phase in Allen-Cahn equation is sharper than one in Cahn-Hilliard equation.

Example 4.2.2 We choose wave crest $a = 0.5$ and wave trough $b = -0.5$ such that the total mass of initial data is almost zero. The evolution of phase function are shown in Fig.(23,24), which the time increases from right to left. Fig.(25,26) are the evolution of mass and energy, respectively, with the time increasing from left to right. Note that the initial mass is almost zero, the evolution of the Allen-Cahn equation still keeps the phase separation after long time calculation. But the variation of mass is still large.

Example 4.2.3 We choose wave crest $a = 0.2$ and wave trough $b = -0.8$ such that the total mass of initial data is negative. The evolution of phase function are shown in Fig.(27,28), which the time increases from right to left. Fig.(29,30) are the evolution of mass and energy, respectively, with the time increasing from left to right. Again, we note that the mass does not preserved in the Allen-Cahn equation. The phase function tends to -1.0 after a short period of time.

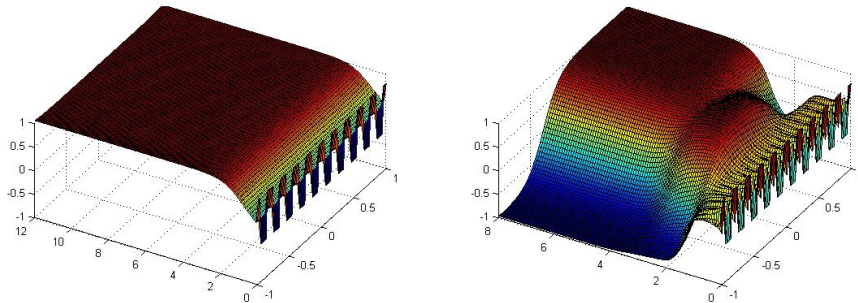


Figure 19: The evolution of phase function of Allen-Cahn (left, CN-AB method, $t=0$ to 12) and Cahn-Hilliard (right, CN-AB method, $t=0$ to 12) equations, max 0.8, min -0.2

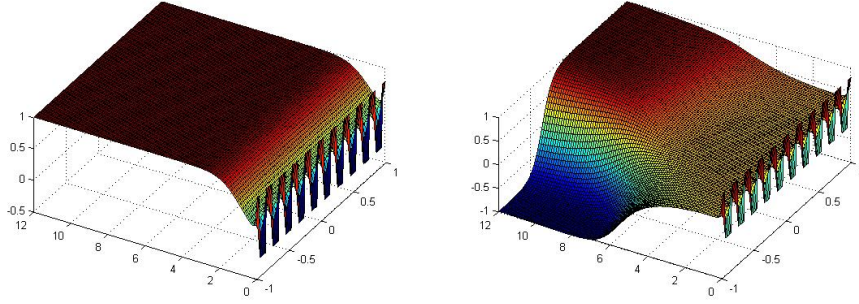


Figure 20: The evolution of phase function of Allen-Cahn (left, GS method, $t=0$ to 12 and right, GS method with mass-conservation, $t=0$ to 12) equation

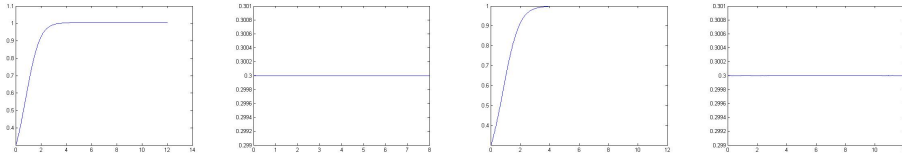


Figure 21: The evolution of mass of Allen-Cahn (left, CN-AB method, $t=0$ to 12, mid-right, GS method, $t=0$ to 12, and right, GS method with mass-conservation, $t=0$ to 12) and Cahn-Hilliard (mid-left, CN-AB method, $t=0$ to 12) equations, initial mass 0.3

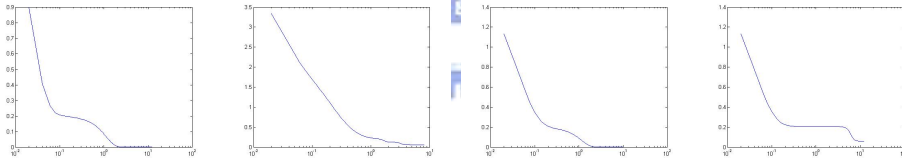


Figure 22: The evolution of energy of Allen-Cahn (left, CN-AB method, $t=0$ to 12, mid-right, GS method, $t=0$ to 12, and right, GS method with mass-conservation, $t=0$ to 12) and Cahn-Hilliard (mid-left, CN-AB method, $t=0$ to 12) equations, log-plot

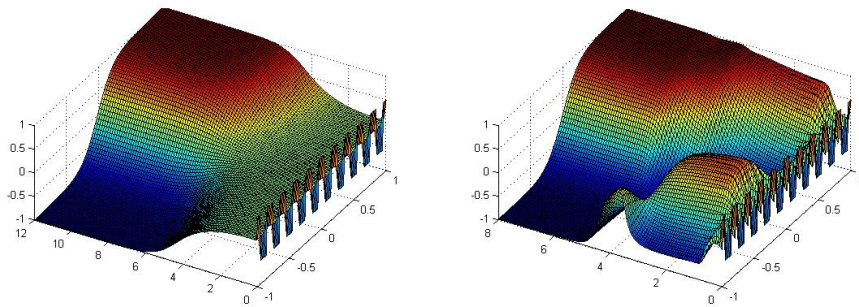


Figure 23: The evolution of phase function of Allen-Cahn (left, CN-AB method, $t=0$ to 12) and Cahn-Hilliard (right, CN-AB method, $t=0$ to 8) equations, max 0.5, min -0.5

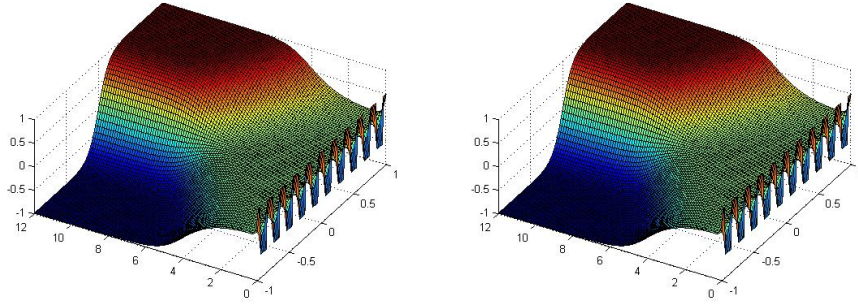


Figure 24: The evolution of phase function of Allen-Cahn (left, GS method, $t=0$ to 12 and right, GS method with mass-conservation, $t=0$ to 12) equation

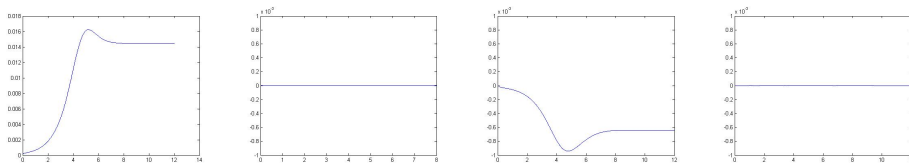


Figure 25: The evolution of mass of Allen-Cahn (left, CN-AB method, $t=0$ to 12, mid-right, GS method, $t=0$ to 12, and right, GS method with mass-conservation, $t=0$ to 12) and Cahn-Hilliard (mid-left, CN-AB method, $t=0$ to 8) equations, initial mass 0.0

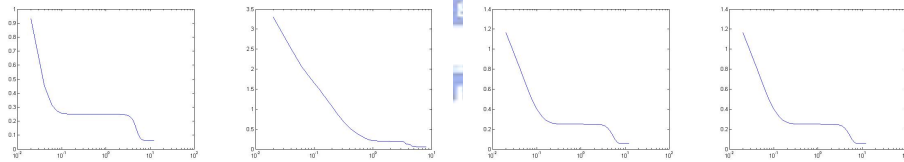


Figure 26: The evolution of energy of Allen-Cahn (left, CN-AB method, $t=0$ to 12, mid-right, GS method, $t=0$ to 12, and right, GS method with mass-conservation, $t=0$ to 12) and Cahn-Hilliard (mid-left, CN-AB method, $t=0$ to 8) equations, log-plot

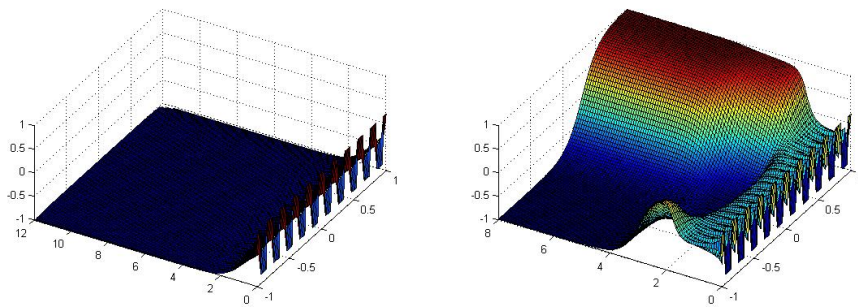


Figure 27: The evolution of phase function of Allen-Cahn (left, CN-AB method, $t=0$ to 12) and Cahn-Hilliard (right, CN-AB method, $t=0$ to 8) equations, max 0.5, min -0.5

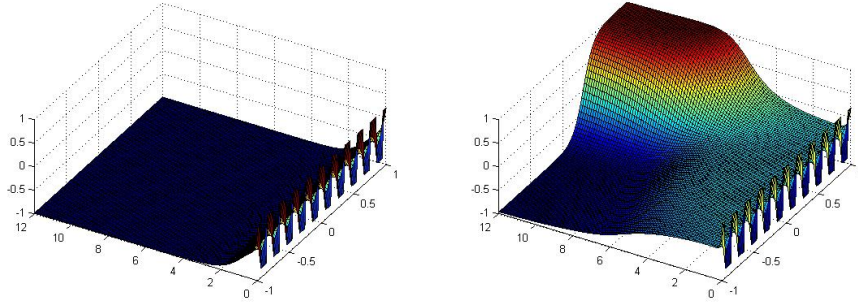


Figure 28: The evolution of phase function of Allen-Cahn (left, GS method, $t=0$ to 12 and right, GS method with mass-conservation, $t=0$ to 12) equation

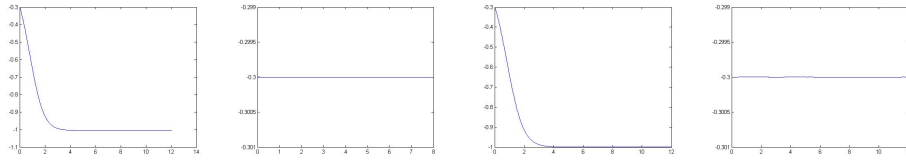


Figure 29: The evolution of mass of Allen-Cahn (left, CN-AB method, $t=0$ to 12, mid-right, GS method, $t=0$ to 12, and right, GS method with mass-conservation, $t=0$ to 12) and Cahn-Hilliard (mid-left, CN-AB method, $t=0$ to 8) equations, initial mass 0.0

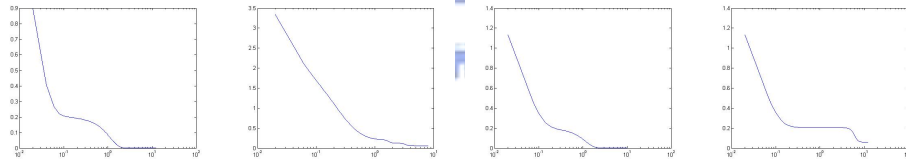


Figure 30: The evolution of energy of Allen-Cahn (left, CN-AB method, $t=0$ to 12, mid-right, GS method, $t=0$ to 12, and right, GS method with mass-conservation, $t=0$ to 12) and Cahn-Hilliard (mid-left, CN-AB method, $t=0$ to 8) equations, log-plot

5 Applications of the Allen-Cahn and Cahn-Hilliard equations

5.1 Mixture of Two Incompressible Fluids

In computation of mixture of two incompressible fluids, instead of taking the interface into consideration, we adapt our phase field model into the Navier-Stokes equation. From works of Jie Shen et al. [17] and [10], we derive the full model as below. the equation of momentum can be written as following :

$$\rho(\mathbf{u}_t + (\mathbf{u} \cdot \nabla)\mathbf{u}) = -\nabla p + \nabla \cdot \sigma + \mathbf{f} \quad (29)$$

where ρ is the density, \mathbf{u} is the velocity, p is the pressure, \mathbf{f} is the buoyancy force, and σ is the stress tensor, including viscosity and induced elasticity. By taking into account the competition between the kinetic energy and the elastic energy, we have

$$\nabla \cdot \sigma = \nabla \cdot [\nu(\nabla \mathbf{u} + (\nabla \mathbf{u})^t)] - \lambda \mu \nabla \phi \quad (30)$$

where ν is the dynamic viscosity coefficient, and $\mu \nabla \phi$ is the induced elastic stress due to the mixing energy, with μ written as

$$\mu = \epsilon^2 \Delta \phi + f(\phi) \quad (31)$$

And λ corresponds to the ration between the kinetic energy and the elastic energy. In this case, it is related to the surface tension coefficients. Suppose two fluids have different density ρ_1 and ρ_2 , with relatively small difference between them. By imposing the classical Boussinesq approximation, we have

$$\begin{aligned} \rho(\mathbf{u}_t + (\mathbf{u} \cdot \nabla)\mathbf{u}) + \nabla p - \nabla \cdot [\nu(\nabla \mathbf{u} + (\nabla \mathbf{u})^t)] + \lambda(\epsilon^2 \Delta \phi + f(\phi)) \nabla \phi &= \mathbf{f} \\ \nabla \cdot \mathbf{u} &= 0 \end{aligned} \quad (32)$$

with the the buoyancy force \mathbf{f} defined by

$$\mathbf{f} = -[(1 + \phi)(\rho_1 - \rho_0) + (1 - \phi)(\rho_2 - \rho_0)]g_0 \quad (33)$$

where $\rho_0 = (\rho_1 + \rho_2)/2$, g_0 is the gravity force.

And the phase field part is written as

$$\begin{aligned} \phi_t + (\mathbf{u} \cdot \nabla)\phi &= \gamma(\epsilon^2 \Delta \phi + f(\phi)) + \sigma(t) \\ \frac{d}{dt} \int_{\Omega} \phi dx &= 0 \end{aligned} \quad (34)$$

where γ represents the elastic relaxation time.

5.2 Numerical Scheme for Coupled System

The first part is to compute the Navier-stokes equation. We use a three-step scheme, from Tseng's work [13].

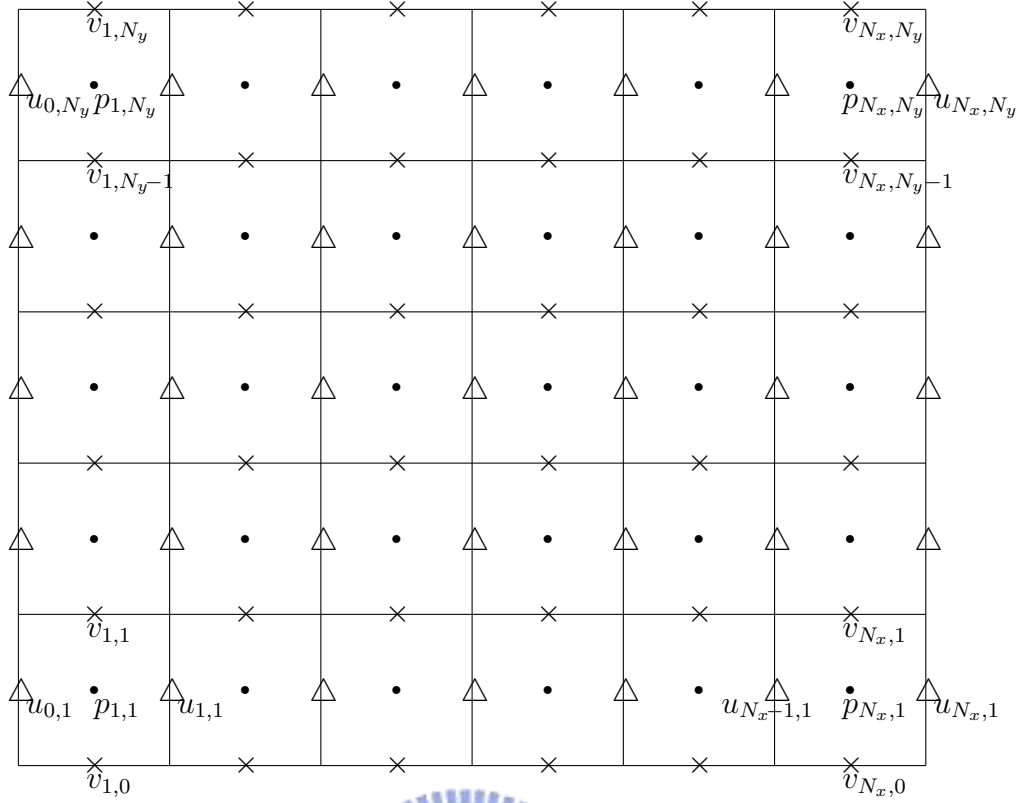


Figure 31: The computational domain Ω using staggered Grid with mesh size h , phase function ϕ is defined at the same position of pressure p

Step 1. Prediction step. We solve \mathbf{u}^* explicit where

$$\frac{\mathbf{u}^* - \mathbf{u}^n}{\Delta t} + (\mathbf{u} \cdot \nabla) \mathbf{u}^{n+\frac{1}{2}} + \nabla p^{n-\frac{1}{2}} = \frac{\nu}{2} \Delta \mathbf{u}^n - \lambda (\Delta \phi + f(\phi))^n \nabla \phi^n + \mathbf{f} \quad (35)$$

And $\tilde{\mathbf{u}}^{n+1}$ by a fast Poisson solver

$$\frac{\tilde{\mathbf{u}}^{n+1} - \mathbf{u}^*}{\Delta t} = \frac{\nu}{2} \Delta \tilde{\mathbf{u}}^{n+1} \quad (36)$$

Note that the advection term $(\mathbf{u} \cdot \nabla) \mathbf{u}^{n+\frac{1}{2}}$ is approximated by the extrapolation

$$\frac{3}{2} (\mathbf{u} \cdot \nabla) \mathbf{u}^n - \frac{1}{2} (\mathbf{u} \cdot \nabla) \mathbf{u}^{n-1}$$

We shall explain this in detail. In the first component of the vector field, we have these terms of the space discretization

$$\begin{aligned} \left(u \frac{\partial u}{\partial x} + v \frac{\partial u}{\partial y} \right)^{n+\frac{1}{2}} &= \frac{3}{2} \left(u_{i,j}^n \frac{u_{i+1,j}^n - u_{i-1,j}^n}{2\Delta x} + v_{stag}^n \frac{u_{i,j+1}^n - u_{i,j-1}^n}{2\Delta y} \right) \\ &\quad - \frac{1}{2} \left(u_{i,j}^{n-1} \frac{u_{i+1,j}^{n-1} - u_{i-1,j}^{n-1}}{2\Delta x} + v_{stag}^{n-1} \frac{u_{i,j+1}^{n-1} - u_{i,j-1}^{n-1}}{2\Delta y} \right), \\ \frac{\partial p^{n-\frac{1}{2}}}{\partial x} &= \frac{p_{i+1,j}^{n-\frac{1}{2}} - p_{i,j}^{n-\frac{1}{2}}}{\Delta x}, \\ \Delta u^n &= \frac{u_{i+1,j}^n - 2u_{i,j}^n + u_{i-1,j}^n}{\Delta x^2} + \frac{u_{i,j+1}^n - 2u_{i,j}^n + u_{i,j-1}^n}{\Delta y^2}, \end{aligned}$$

and the interpolation

$$v_{stag} = \frac{1}{4} (v_{i,j} + v_{i,j-1} + v_{i+1,j} + v_{i+1,j-1})$$

from v -grid to u -grid. The second component is similar.

Step 2. Projection step. We correct the velocity \mathbf{u} to satisfy the divergence free condition. and we also update the pressure p . According to the Helmholtz-Hodge decomposition, we obtain

$$\begin{aligned} \tilde{\mathbf{u}}^{n+1} &= \mathbf{u}^{n+1} + \Delta t \nabla \psi \\ \nabla \cdot \mathbf{u}^{n+1} &= 0 \end{aligned} \quad (37)$$

for some function ψ . This means that we want to project $\tilde{\mathbf{u}}^{n+1}$ to the divergence free one, \mathbf{u}^{n+1} . Taking divergence on both sides, we have

$$\begin{aligned} \frac{\nabla \cdot \tilde{\mathbf{u}}^{n+1}}{\Delta t} &= \Delta \psi \\ \frac{\partial \psi}{\partial n} &= 0 \text{ where } x \in \partial \Omega \end{aligned}$$

Note that we need to compute the divergent term $\nabla \cdot \tilde{\mathbf{u}}^{n+1}$ on the p -grid, solve the Laplace equation of ψ , and then obtain \mathbf{u}^{n+1} .

Step 3. Correction step. Since

$$\nabla p^{n+\frac{1}{2}} = \nabla p^{n-\frac{1}{2}} + \nabla \psi - \frac{\nu \Delta t}{2} \nabla (\Delta \psi)$$

We obtain

$$p^{n+\frac{1}{2}} = p^{n-\frac{1}{2}} + \psi - \frac{\nu}{2} \nabla \cdot \tilde{\mathbf{u}}^{n+1}$$

It can be obtained by substituting (37) into the summation of (35) and (36).

The second part is the phase field models. We modified the CN-AB scheme for Allen-Cahn equation as below:

$$\begin{aligned} \frac{\tilde{\phi}^{n+1} - \phi^n}{\Delta t} + (\mathbf{u} \cdot \nabla) \phi^{n+\frac{1}{2}} &= \frac{\epsilon^2}{2} (\Delta \tilde{\phi}^{n+1} + \Delta \tilde{\phi}^n) \\ &+ \frac{1}{2} (-2\tilde{\phi}^{n+1} - 2\phi^n + 3(3\phi^n - (\phi^n)^3) - (3\phi^{n-1} - (\phi^{n-1})^3)) \end{aligned}$$

with a correction step for mass conservation:

$$\rho(n+1) = \frac{\sum \tilde{\phi}^{n+1} \Delta x}{\text{vol}(\Omega)} - M(\phi) = \tilde{\phi}^{n+1} - \rho(n+1)$$

Since the velocity \mathbf{u}^{n+1} is computed in the first part, we use the extrapolation

$$\mathbf{u}^{n+1} \cdot \left(\frac{3}{2} \nabla \phi^n - \frac{1}{2} \nabla \phi^{n-1} \right)$$

to the term $(\mathbf{u} \cdot \nabla) \phi^{n+\frac{1}{2}}$ in a similar way in computation of advection term in Navier-Stokes equation.

5.3 Computing Mixture Problems Using Phase Field Models

Here we present an example of computing mixture problems using phase field models. This is a modified case from Yang, et al. [17]. Consider the retraction of a rectangular filament of width 0.2 and height 2.0 placed at center of the calculation domain $[-1, 1] \times [0, 6]$, filled with another ambient fluid. Suppose both fluids have the same density and viscosity. Set $\phi = 1$ inside the filament and $\phi = -1$ in the ambient fluid. The parameters are given as following:

$$\gamma = 1.0, \epsilon = 0.02, \lambda = 0.5, \nu = 1.0, g_0 = 0, \rho_1 = \rho_2 = 1.0 \quad (38)$$

with number of grid point 128×128 , $\delta t = 0.01$. During computation, pressure p and phase function ϕ is defined on cell center, while the velocity $\mathbf{u} = (u, v)$ is calculated on cell interface. We use the **CN-AB method with mass-conservation** to compute the phase field models.

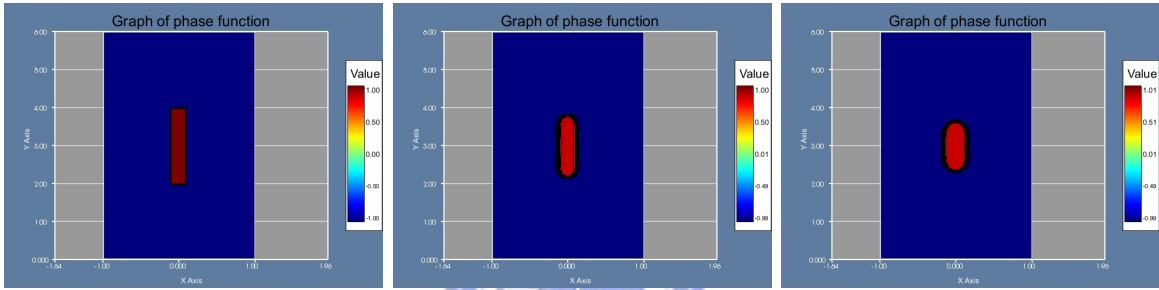


Figure 32: The contour profile of phase function when $t=0, 50, 100$, from left to right

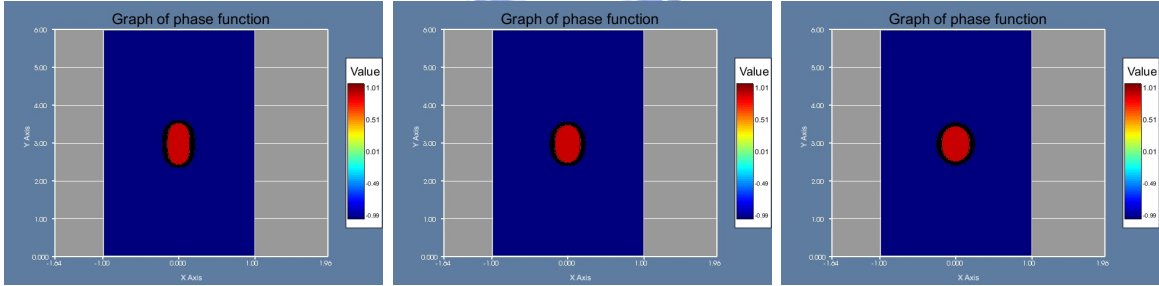


Figure 33: The contour profile of phase function when $t=125, 150, 175$, from left to right

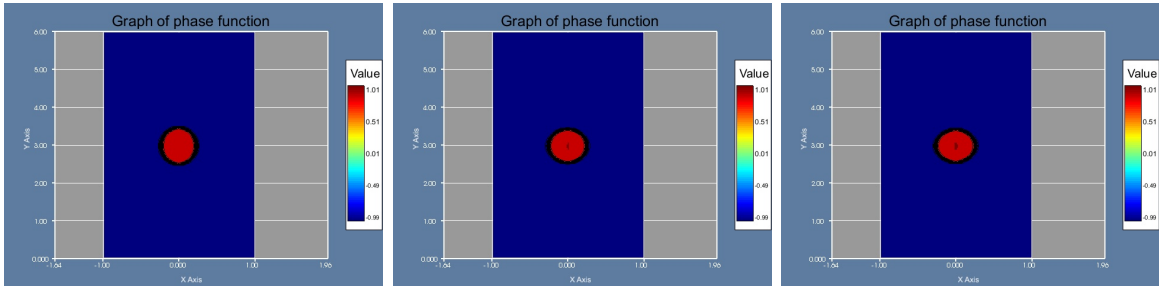


Figure 34: The contour profile of phase function when $t=200, 250, 300$, from left to right

We can observe that, with initial velocity set to be zero and pressure assigned constant, the surface tension produces the movement of the interface. The filament contracts and forms a single droplet slowly in a long-time period.

6 Conclusion

We propose simple finite difference schemes with fast and stable computations for the Allen-Cahn equation with solving tri-diagonal matrices. We also deal this with the Cahn-Hilliard equation in a similar way. We introduce a special splitting method for the Allen-Cahn equation in advantage of applying fast Fourier transform. Mass-conservation modification for the Allen-Cahn equation is provided. And we apply these methods to compute the mixture problem of two incompressible fluids.

References

- [1] Allen, S.M., Cahn, J.W. (1976). Mechanisms of phase transformations within the miscibility gap of Fe-Rich Fe-Al alloys. *Acta Meta.*, 24, 425–437
- [2] Badalassi, V.E., Cenicerros, H.D., Banerjee, S. (2003). Computation of multiphase systems with phase field models. *J. Comp. Phys.*, 190, 371–397
- [3] Cahn, J.W., Hilliard, J.E. (1958). Free energy of a nonuniform system. I. Interfacial free energy. *J. chem. phys.*, 28, 258–267.
- [4] Carr, J., Pego, R.L. (1989). Metastable Patterns in solutions of $U_t = \epsilon^2 U_{xx} - f(U)$. *Comm. Pure Appl. Math.*, 42, 523–576
- [5] Elliot, C.M., French, D.A. (1987). Numerical studies of the Cahn-Hilliard equation for phase separation. *IMA J. Appl. Math.*, 38, 97–128.
- [6] Elliot, C.M., French, D.A., Milner, F.A. (1989). A second order splitting method for the Cahn-Hilliard equation. *Numer. Math.*, 54, 575-590
- [7] Eyre, D.J. (1998). An unconditionally stable one-step scheme for gradient systems. Preprint.
- [8] Furihata, D. (2001). A stable and conservative finite difference scheme for the Cahn-Hilliard equation. *Numer. Math.*, 87, 675–699.
- [9] Furihata, D. (2003). A stable, convergent, conservative and linear finite difference scheme for the Cahn-Hilliard equation. *Japan J. Indust. Appl. Math.*, 20, 65–85
- [10] Liu, C., Shen, J. (2003). A phase field model for the mixture of two incompressible fluids and its approximation by a Fourier-spectral method. *Phys. D*, 179, 211–228
- [11] Nie, Q., Zhang, Y., Zhao, R. (2005). Efficient semi-implicit schemes for stiff systems. *J. Comp. Phys.*, 214, 521–537
- [12] Trefethen, L.N. (2000). Spectral methods in MATLAB, pp.137-141. SIAM.

- [13] Tseng, H. (2006). Numerical methods and applications for immersed interface problems. Master Thesis.
- [14] Vollmayr-Lee, B.P., Rutenberg, A.D. (2003). Fast and accurate coarsening simulation with an unconditionally stable time step. *Phys. Rev. E*, 68, 066703
- [15] Ward, M.J. (1996). Metastable bubble solutions for the Allen-Cahn equation with mass conservation. *SIAM J. Appl. Math.*, 56, 1247–1279.
- [16] Ward, M.J., Stafford, D. (1999). Metastable dynamics and spatially inhomogeneous equilibria in dumbbell-shaped domains. *Stud. Appl. Math.*, 103, 51–73
- [17] Yang, X., Feng, J.J., Liu, C., Shen, J. (2006). Numerical simulations of jet pinching-off and drop formation using an energetic variational phase-field method. *J. Comp. Phys.*, 218, 417–428

